NASA TN D-776

TECHNICAL NOTE

D-776

A WIND-TUNNEL INVESTIGATION OF A 4-FOOT-DIAMETER DUCTED FAN MOUNTED ON THE TIP OF A SEMISPAN WING

By Paul F. Yaggy and Kenneth W. Mort

Ames Research Center
Moffett Field, Calif.

NATIONAL AERONAUTICS AND SPACE ADMINISTRATION
WASHINGTON
March 1961

NATIONAL AERONAUTICS AND SPACE ADMINISTRATION

TECHNICAL NOTE D-776

A WIND-TUNNEL INVESTIGATION OF A 4-FOOT-DIAMETER DUCTED FAN MOUNTED ON THE TIP OF A SEMISPAN WING

By Paul F. Yaggy and Kenneth W. Mort

SUMMARY

Power, wing angle of attack, and the angle of the duct relative to the wing were varied to achieve a specified lift and thrust for a forward velocity range from 0 to 140 knots. In this manner a so-called transition program of steady-state conditions was defined over the velocity range.

It was found that large pitch-up moments resulted when the ducted fan was operated at an angle of attack to the air stream. A deflected vane installed in the high-energy air at the duct exit was helpful in reducing these pitch-up moments. Large downwash angles were induced by the ducted fan at a selected horizontal-tail location.

The possibility of using guide vanes in the duct inlet to vary thrust for the purpose of roll control at low forward speeds was examined. The maximum incremental thrust available at zero forward velocity was found to be 11 percent of the total thrust required at that speed.

INTRODUCTION

Experimentally obtained information concerning the performance of full-scale ducted fans suitable for lifting and propelling VTOL aircraft has been very meager. Therefore, an investigation of a 4-foot-diameter ducted fan mounted on the tip of a semispan wing has been performed in the Ames 40- by 80-Foot Wind Tunnel.

The tests were directed primarily toward the determination of a transition program for level, unaccelerated flight from hover to airplane flight, and the effects of the ducted fan on aircraft control requirements during this transition. Herein, a "transition program" is defined as the variations of the power required, the wing angle of attack, and the duct angle relative to the wing chord which would be required to perform the transition. Because of the restricted objective, the results represent only an exploratory investigation of this wing-duct configuration and its problems and not an exhaustive study.

The information that existed prior to these tests indicated that large pitching moments occurred when ducted fans were operated at large angles of attack to the air stream. Therefore, provision was made to study the effectiveness of a vane in the duct exit as a means of reducing the magnitude of these moments. Surveys of the air flow at a representative tail-plane location were made also to determine the influence of the ducted fan on the performance of a horizontal tail.

Roll control on a VTOL aircraft of this type may be obtained in hovering and low-speed flight by differentially varying the thrust of the ducted fans on the wing tips. Therefore, the investigation included tests to determine the effectiveness of two guide vane configurations in the duct inlet as a means of varying thrust.

NOTATION

A	fan area, ft^2
b	fan blade chord, in.
$\bar{c}$	wing mean aerodynamic chord, ft
C_D	drag coefficient, $\frac{D}{qS}$
C_{l_i}	fan design lift coefficient, $\frac{l_i}{qb}$
C_L	lift coefficient, $\frac{L}{qS}$
C_m	pitching-moment coefficient, $\frac{M}{qS\bar{c}}$
d	fan diameter, ft
D	drag, parallel to the tunnel air stream, lb
F_N	duct normal force, perpendicular to the thrust axis of the duct, lb
h	fan blade thickness, in.
l_i	blade section design lift, lb
L	lift, perpendicular to the free air stream, lb
m	pitching moment about center of gravity, ft-lb
N	fan rotational speed, rpm
q	free-stream dynamic pressure, lb/ft^2

r	radial distance from duct center line, ft
R	fan radius, ft
S	wing area, ft^2
SHP	shaft horsepower
T	duct thrust, parallel to the thrust axis of the duct, lb
V_∞	free-stream velocity, knots
X	chordwise distance from duct leading edge, positive aft, in.
α_w	wing angle of attack, deg
β	fan blade angle measured at tip, deg (unless otherwise stated)
δ_d	duct angle relative to wing chord line, deg
δ_V	inlet guide vane angle (shown positive in fig. 12), deg
δ_F	exit vane angle (positive trailing edge down), deg
δ_T	exit vane flap angle (positive trailing edge down), deg
ϵ	downwash angle, the angle between the local air flow and the wing chord plane (positive downward), deg

MODEL AND APPARATUS

General Characteristics

The ducted fan selected for the investigation was an exact duplicate of those used on the Doak VZ-4DA airplane. The semispan wing panel upon which the duct was mounted had the same geometric dimensions as the left wing panel of that airplane. The general arrangement of the ducted fan and wing mounted in the wind tunnel for testing is shown in figure 1. Dimensions of the fan and wing are shown in figure 2 and in tables I and II. As may be seen in these figures, a reflection plane was attached to the inboard end of the wing at the longitudinal plane of symmetry. All structure exposed to the air stream below this plane was isolated from the force-measuring system; that is, only forces and moments on the ducted fan, wing, and reflection plane were recorded.

Fan

The eight-bladed fan had a fixed blade pitch of 15° at the tip. The blades were of solid glass fiber construction. The clearance between the fan tip and the duct was approximately 0.030 inch. Blade plan-form curves are shown in figure 3; other pertinent dimensions are shown in table I.

Inlet Guide Vanes

Two sets of inlet guide vanes were tested, one set of 7 vanes and a second set of 14 vanes. The angular range of movement of the vanes relative to the position at which the vane chord was alined with the thrust axis was ±10° for the 7-vane configuration and -10° to +30° for the set of 14 vanes. Pertinent characteristics and dimensions of the vanes are shown in table I.

Stators

Nine stators were used in the duct aft of the fan to remove rotation from the exit flow. Eight of the stators had 6-inch-chord NACA 0008.4 airfoil shapes superposed on an NACA $a = 0.4$ mean line. The ninth vane, which housed the fan drive shaft, had a 9-inch-chord NACA 0017 airfoil shape on the same mean line. Other characteristics of the stators are given in table I.

Duct Exit Vane

The vane was constructed with a 25-percent-chord plain flap. The vane deflection range was from 0° to 30° and the flap deflection range was from 0° to 20°. Pertinent dimensions and characteristics of the vane are shown in table I and figure 1(b).

Fan Drive System

The fan was driven by a 1000-horsepower electric motor through a shaft within the wing. The motor speed could be varied continuously from 0 to 6600 revolutions per minute. Power input to the motor was recorded on a polyphase wattmeter. The readings were corrected for motor efficiency.

Instrumentation

Forces and moments on the ducted fan and wing combination were measured on the wind-tunnel six-component balance. Strain gages on the duct trunnion support tube measured the duct thrust, duct normal force, and duct pitching moment. Directional pitot-static pressure probes were used on a survey apparatus to measure the flow at a representative tail-plane location corresponding to the quarter-chord line of the horizontal tail on the Doak VZ-4DA airplane. The probes indicated both the dynamic pressure and the direction of the local air flow.

TESTS

Wing and Wing-Duct Characteristics At Zero Power

In order to provide some basic information on the aerodynamics of the straight- and ring-wing combination, tests of the wing alone and wing-duct combination were made with zero power input to the fan. Under these conditions the only force on the fan was its windmilling drag, and it was presumed that the presence of the fan had only a small effect upon the duct aerodynamics. Data were obtained at wing angles of attack from 0° to 20° for 0° duct angle and at duct angles from 0° to 90° for 0° wing angle of attack.

Simulation of Transition Flight

As noted previously, the tests were directed primarily toward the determination of a transition program from hover to airplane flight, and the effects of the duct on airplane control requirements during this transition. As a basis for these tests, the following airplane characteristics were assumed: weight, 3100 pounds; maximum shaft horsepower, 800; drag of components other than the duct and wing, 1.92 pounds per pound per square foot of free-stream dynamic pressure (accounting for the fuselage and other appendages); and a horizontal-tail quarter-chord line located as shown in figure 2. For the semispan model the appropriate values were halved.

The tests were conducted to find a balance of forces (lift equals weight, thrust equals drag) at several airspeeds by varying both the duct angle relative to the wing and the fan power while the wing angle of attack was held constant. Wing angles of attack of 2° and 6° and forward speeds from 0 to 140 knots were investigated.

Effectiveness of the Duct Exit Vane

The same test conditions were repeated with the exit vane attached to the duct to determine the effects of the vane on pitching moment, power, and duct angle setting. The vane was deflected 0°, 10°, 20°, and 30° with the flap undeflected. The vane was also tested with 10° vane deflection and 20° flap deflection.

Flow at the Horizontal-Tail Location

During the tests described above, measurements were made simultaneously of the direction and magnitude of the air flow at the quarter-chord location of the assumed horizontal tail.

Effectiveness of the Inlet Guide Vanes

Tests of both the 7 and 14 vane configurations were made at 0, 20, and 30 knots forward speed. The inlet vane angle was varied for constant fan rotational speeds to determine its effect on thrust and power. The tests were made at force balance conditions.

REDUCTION OF DATA

All data presented in this report are for the semispan model. Coefficients are based on the model wing area.

Force Balance Conditions

The data obtained during the tests were intended to bracket the force balance conditions closely, so that with minor interpolation, these conditions could be defined. Generally, this objective was realized, although, at speeds of 100 knots and higher, more gross interpolation and some extrapolation was required. Because of the required interpolations, no test points are shown on the figures presenting the variation of test parameters with forward speed. A typical interpolation is shown in appendix A.

Duct Trunnion Strain-Gage Data

The thrust gages were directly calibrated in pounds of force and required no corrections. The normal-force and pitching-moment gages were also calibrated in pounds and foot pounds, respectively, but it was necessary to correct the readings for torque reactions in the fan drive gear box. The torque reactions were computed from the power input data and were subtracted from the values indicated by the strain gages. The gage system failed after tests at 80 knots; therefore, no data at speeds above this value are presented.

Accuracy of Measuring Devices

The various measuring devices used were accurate within the following limits. These values include errors involved in reading and reducing the data as well as in the accuracy of the device itself.

Duct angle	$\pm 0.2^{\circ}$
Lift	±10 pounds
Drag	±2 pounds
Pitching moment	±30 foot-pounds
Fan rotational speed	±30 rpm
Shaft horsepower	±10 horsepower

RESULTS AND DISCUSSION

Wing and Wing-Duct Aerodynamic Characteristics at Zero Fan Power Input

The lift, drag, and pitching-moment coefficients for the wing alone and the wing-duct combination at zero fan power input are shown in figure 4. During the tests, the duct thrust axis was maintained parallel to the wing chord line. The effect of the presence of the duct on the over-all lift is seen to be sizable, nearly doubling the lift coefficient of the wing alone. The effect of the duct on the longitudinal stability is seen to be somewhat destabilizing at the higher lift values.

Figure 5 presents the lift, drag, and pitching-moment coefficients for the wing-duct combination with the wing at 0° angle of attack and the duct thrust axis varied from 0° to 90° angle of attack. Again, the input power to the fan was zero.

Investigation of Transition Program From Hover to Airplane Flight

The variations of duct angle, fan rotational speed, and power required for force balanced conditions during transition are shown in figure 6 as functions of forward velocity for wing angles of attack of 2° and 6°. Comparison of the curves at the two wing angles of attack shows that the power requirement was reduced when the wing angle was increased because more load is carried on the wing.

A 4 4 9

Figure 7 presents the variations of duct thrust, T, and normal force, F_N, with forward speed for the transition programs defined in figure 6.

Figure 8 shows the variations of the pitching moment with forward speed for both the duct and the wing-duct combination operating at the conditions defined in figure 6. The duct moments were measured by the trunnion strain gage simultaneously with moments measured on the tunnel balance for the combination. The differences between the curves for the duct and for the wing-duct combination are due to the wing and any mutual interference effects between the wing and duct. It may be noted that these effects were relatively small and the duct was the primary source of the pitching moment. A comparison of these variations for the two wing angles of attack shows that, in addition to reduced power required, a reduction in pitching moment is also realized at the higher wing angle of attack.

Trim in Pitch During Transition Flight

The downwash angles which were measured at the horizontal-tail location are shown in figure 9 as a function of forward speed; the values of dynamic pressure at this location were essentially free stream. From these results, it is seen that if a horizontal tail with approximately 0° incidence were used in the speed range between 30 and 70 knots, it would add out of trim nose-up moments. Thus, it is indicated that a variable-incidence tail probably would be desirable to reduce the control problem.

The results of the tests with the vane installed in the duct exit are shown in figure 10 for the balanced lift and drag condition at two wing angles of attack. The results indicate a significant reduction in nose-up moment with the exit vane installed. However, the vane had little effect in reducing the downwash angle at the tail location (see fig. 9), and, as a consequence, the desirability of a variable-incidence stabilizer was not eliminated. The corresponding variations of duct angle, fan rotational speed, and power required for the balanced lift and drag condition are shown in figure 11. The change in these characteristics was small compared to the reduction in pitching moments.

A
4
4
9

Lateral Control by Differential Thrust

Figure 12 shows the incremental thrust and power variations as functions of inlet guide vane angle for the 7- and 14-vane configurations at 0, 20, and 30 knots. The zero deflection point is that for force balance at the specified forward speed.

The results indicate that the maximum incremental thrust available for roll control at hover was 11 percent of the total thrust required for force balance. For an airplane of the gross weight being considered herein, the roll control for hover would appear to be marginal according to the requirements set forth in reference 1.

SUMMARY OF RESULTS

A transition program from hover to airplane flight of duct angle and power required for constant wing angles of attack at speeds from 0 to 140 knots has been shown for a semispan wing-duct combination assuming an airplane gross weight of 3100 pounds. The nose-up pitching moments during transition reached a maximum at approximately 45 knots. They appeared to be caused primarily by the duct operating at an angle of attack to the air stream. These moments could be greatly reduced by the use of a deflected vane in the duct exit.

The downwash angles induced by the duct-wing combination at the assumed tail location reached a maximum of 6° at 20 knots. The dynamic pressures remained at free-stream values.

The maximum incremental thrust available for roll control from deflection of the inlet guide vanes was 11 percent of the total thrust at hover conditions.

Ames Research Center
National Aeronautics and Space Administration
Moffett Field, Calif., Jan. 9, 1961

APPENDIX A

PROCEDURE FOR DETERMINING FORCE BALANCE CONDITIONS

Only sufficient data were obtained to define the lift and drag balance at a given airspeed and wing angle of attack. The basic procedure involved determining the partial derivatives of the forces, moments, and power with respect to the fan rotational speed and with respect to the duct angle. The partial derivatives were then used to adjust the nearest data point to the force balance conditions, as in the following example.

Data point	V_∞	α_w	δ_d	N	L	D	M	SHP
1	40	6	61	4100	1592	-24	1189	269
2	40	6	62	4100	1625	-6	1198	269
3	40	6	62	4050	1592	0	1192	258
2-3				$\frac{\partial}{\partial N}$	0.66	-0.12	-0.12	0.22
1-2				$\frac{\partial}{\partial \delta_d}$	33	18	9	0

From the above table, it is apparent that the third data point listed comes the closest to matching the balance conditions of 1550 pounds of lift (1/2 of 3100 pounds) and -12 pounds of drag (1/2 of -1.92q); therefore, $\Delta L = -42$ pounds and $\Delta D = -12$ pounds, where Δ is defined to be the difference between the balance point values and the nearest data point values.

For conditions close to balance:

$$\Delta L = \frac{\partial L}{\partial N}\Delta N + \frac{\partial L}{\partial \delta_d}\Delta\delta_d \qquad (A1)$$

$$\Delta D = \frac{\partial D}{\partial N}\Delta N + \frac{\partial D}{\partial \delta_d}\Delta\delta_d \qquad (A2)$$

$$\Delta M = \frac{\partial M}{\partial N}\Delta N + \frac{\partial M}{\partial \delta_d}\Delta\delta_d \qquad (A3)$$

$$\Delta SHP = \frac{\partial SHP}{\partial N} \Delta N + \frac{\partial SHP}{\partial \delta_d} \Delta \delta_d \qquad (A4)$$

Solving equations (A1) and (A2) simultaneously for ΔN and $\Delta \delta_d$ and substituting in the appropriate values from the above table gives: $\Delta N = -23$ rpm and $\Delta \delta_d = -0.8^\circ$. Values for ΔM and ΔSHP now found using equations (A3) and (A4) are -10 ft-lb and -5 HP, respectively.

It is now possible to define balance.

$$N_{bal} = N + \Delta N = 4050 - 23 = 4027 \text{ rpm}$$

$$\delta_{d_{bal}} = \delta_d + \Delta \delta_d = 62 - 0.8 = 61.2^\circ$$

$$M_{bal} = M + \Delta M = 1192 - 10 = 1182 \text{ ft-lb}$$

$$SHP_{bal} = SHP + \Delta SHP = 258 - 5 = 253 \text{ HP}$$

REFERENCE

1. Anderson, Seth B.: An Examination of Handling Qualities Criteria for V/STOL Aircraft. NASA TN D-331, 1960.

TABLE I.- DIMENSIONS AND CHARACTERISTICS OF VANES

Dimensions	
Duct	
Inside diameter, ft	4
Outside diameter	4 ft 10.5 in.
Chord	2 ft 9 in.
Exit diameter	4 ft 6.3 in.
Diffuser angle, deg	11
Inlet guide vanes	
Chord, in.	3
Number of vanes	
Set 1	7
Set 2	14
Airfoil section	
Set 1	NACA 65A010
Set 2	NACA $65_2$015
Position of vane c/4, percent of duct chord	14.5
Twist, deg	0
Fan	
Plan-form curves	(see fig. 3)
Number of blades	8
Hub to tip diameter ratio	0.333
Position of hub center line, percent of duct chord	29.3
Design static thrust disc loading, psf	150
Design static power disc loading, HP/ft^2	7.96
Blade angle control	fixed pitch
Blade angle at tip, deg	15
Stators	
Number of stators	9
Position of stator c/4, percent of duct chord	49.4
Twist, centerbody to tip, deg	15
Airfoil shape	(see text)
Duct exit vane	
Chord, in.	15
Airfoil section	NACA 0009
Flap chord, percent vane chord	25
Wing	
Airfoil section	NACA 2418
Area, sq ft	48
Semispan, ft	8
Mean aerodynamic chord, ft	6.09
Taper ratio	0.675

TABLE II.- SHROUD AND CENTERBODY COORDINATES

Shroud coordinates tabulated in percent of shroud chord (33.00 in.)			Centerbody coordinates tabulated in percent of centerbody length (71.5 in.)	
Chordwise length, X	Outside radius, r_o	Inside radius, r_i	Length, X	Radius, r
0	81.5	81.5	0	0
.5	83.4	79.6	.5	2.07
.75	83.8	79.0	1.25	3.20
1.25	84.4	78.4	2.50	4.46
2.5	85.4	77.2	5.0	6.17
5.0	86.4	75.8	7.5	7.40
7.5	87.1	74.9	10.0	8.31
10.0	87.6	74.2	15.0	9.68
15.0	88.2	73.3	20.0	10.54
20.0	88.6	72.9	25.0	11.01
25.0	88.6	72.7	25.875[1]	11.06
30.0	88.6	72.7	30.0	11.19
35.0	88.6	72.7	32.57[2]	11.19
40.0	88.6	72.7	40.0	11.19
45.0	88.6	72.7	50.0	11.19
50.0	88.6	72.7	60.0	11.19
55.0	88.6	73.2	70.0	10.49
60.0	88.6	74.1	72.05[3]	10.14
65.0	88.0	75.1	80.0	7.97
70.0	87.4	76.1	83.20	6.77
75.0	86.8	77.1	90.0	4.03
80.0	85.9	78.1	95.0	2.01
85.0	85.2	79.1	100.0	0
90.0	84.3	80.1		
95.0	83.3	81.1		
100.0	82.2	82.0		

[1]Shroud leading-edge position.
[2]Inlet guide vane c/4 line position.
[3]Shroud trailing-edge position.

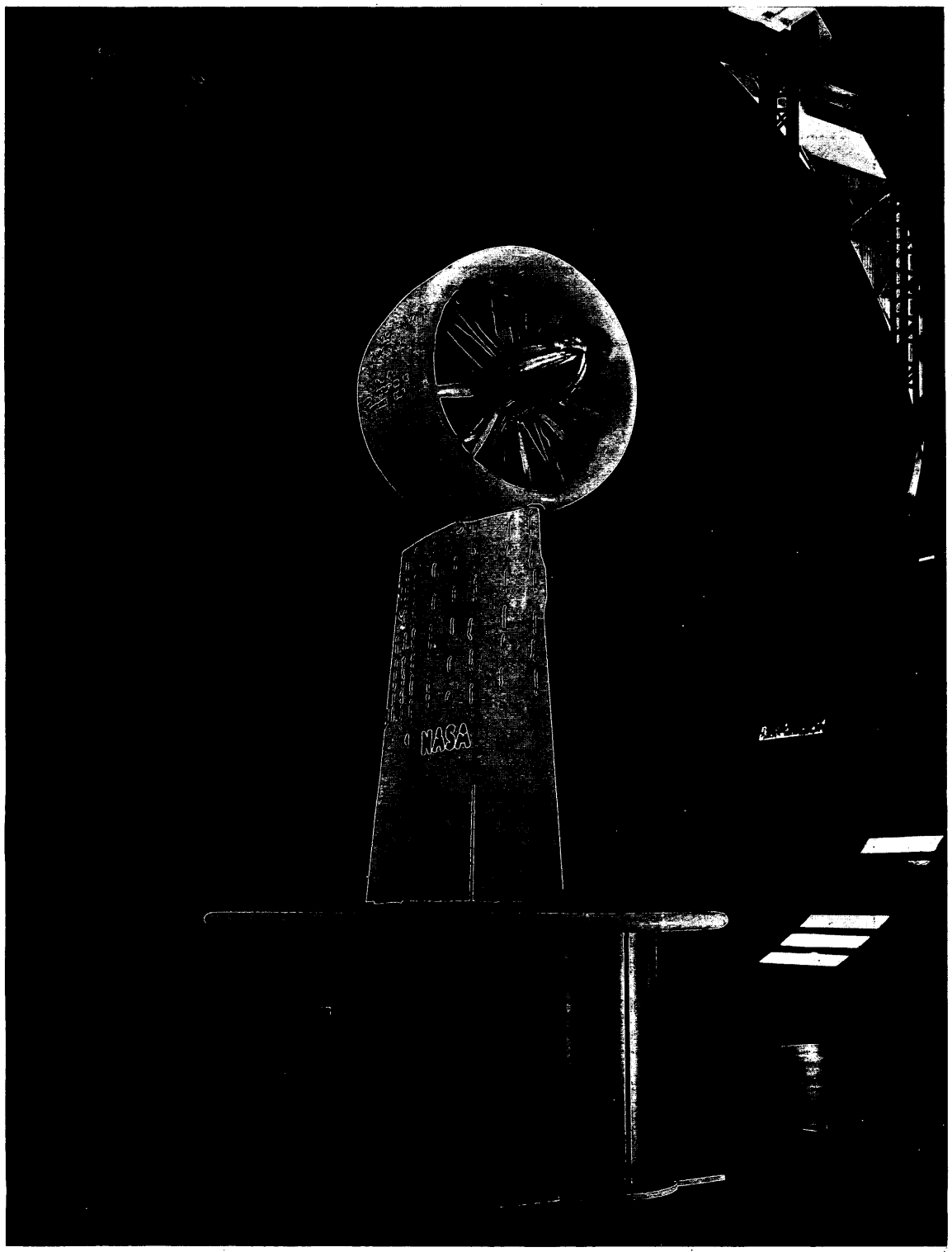

A-25140

(a) Duct at 0°.

Figure 1.- Ducted fan model mounted in the Ames Research Center 40- by 80-foot wind tunnel.

A-25172

(b) Duct at 90°.

Figure 1.- Concluded.

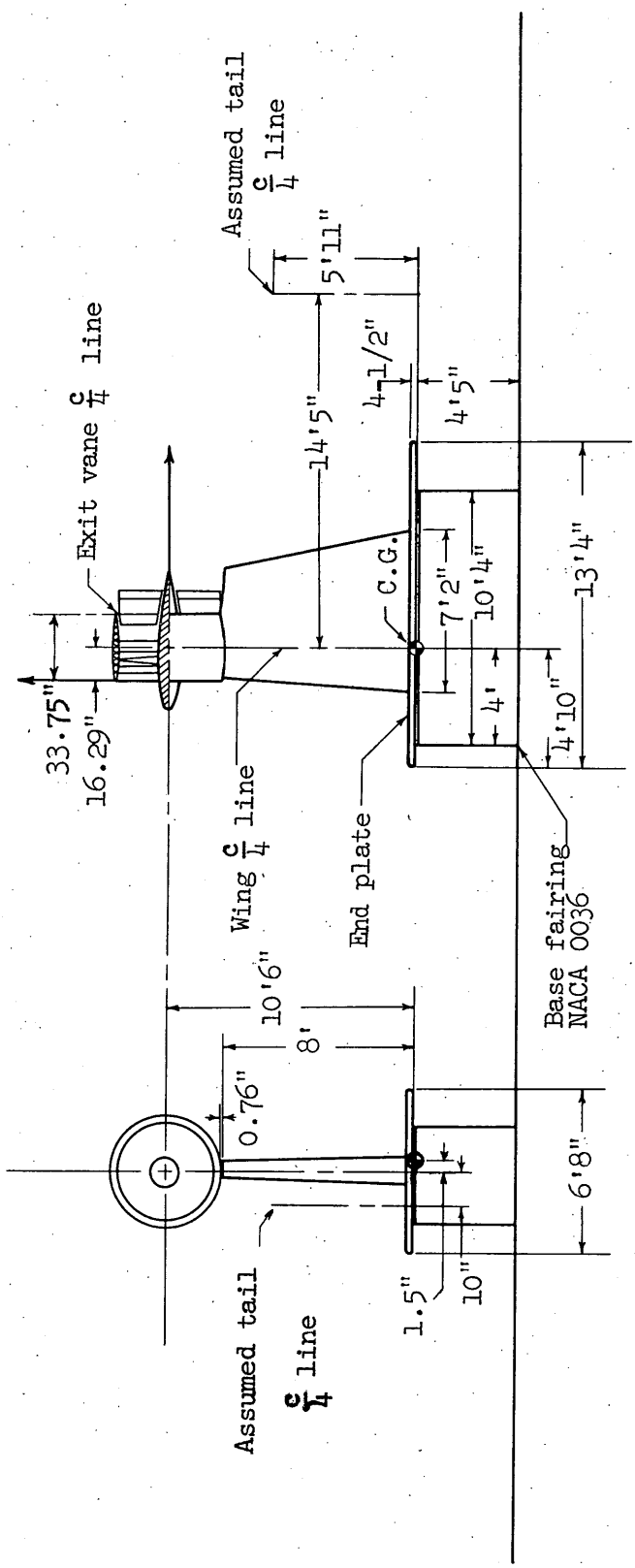

Figure 2.- Basic model dimensions.

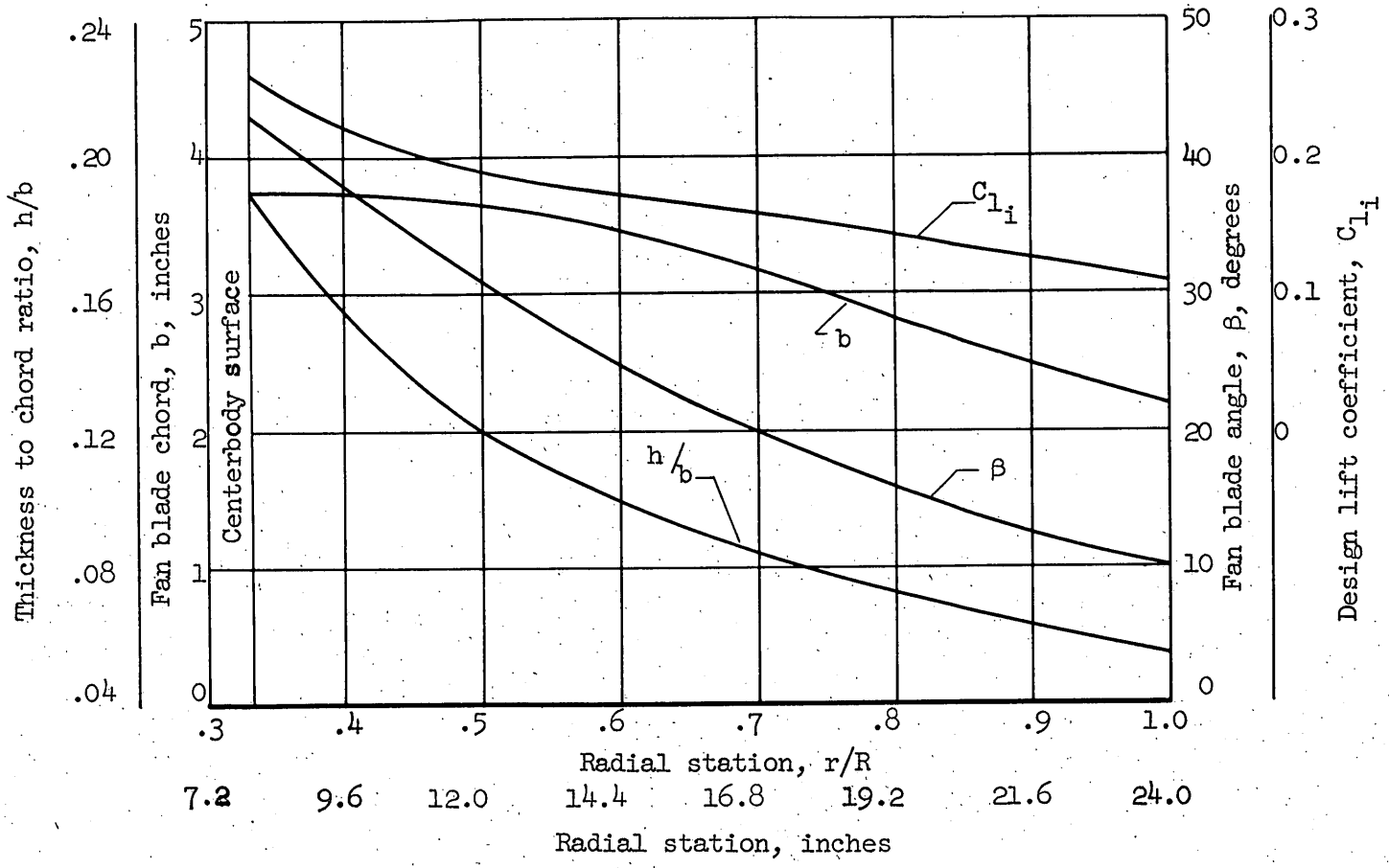

Figure 3.- Fan blade-form curves with the design lift coefficient, blade chord, blade angle, and blade thickness to chord ratio as functions of the radial distance from the duct center.

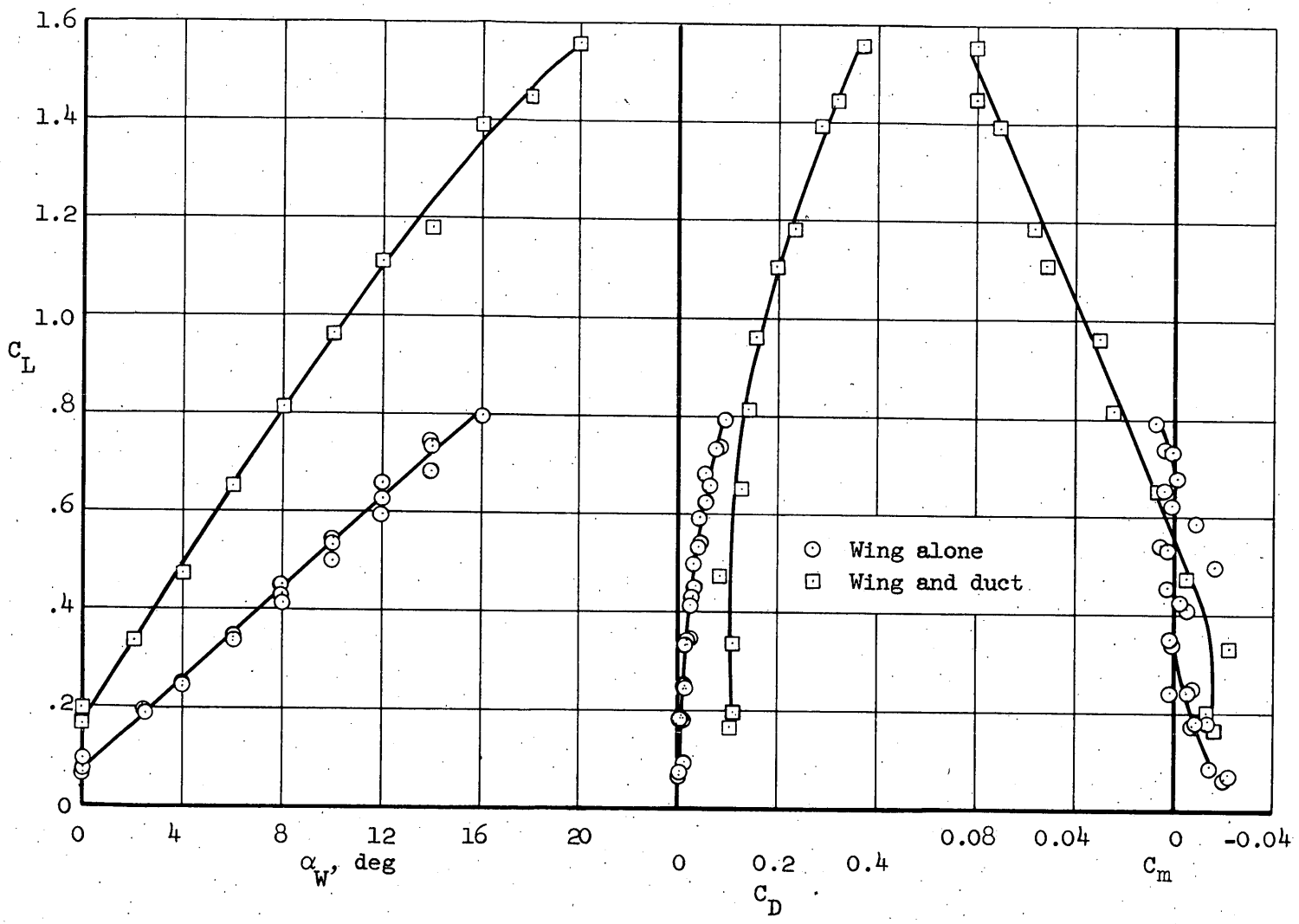

Figure 4.- Aerodynamic characteristics with the duct at 0° relative to the wing chord; zero fan input power.

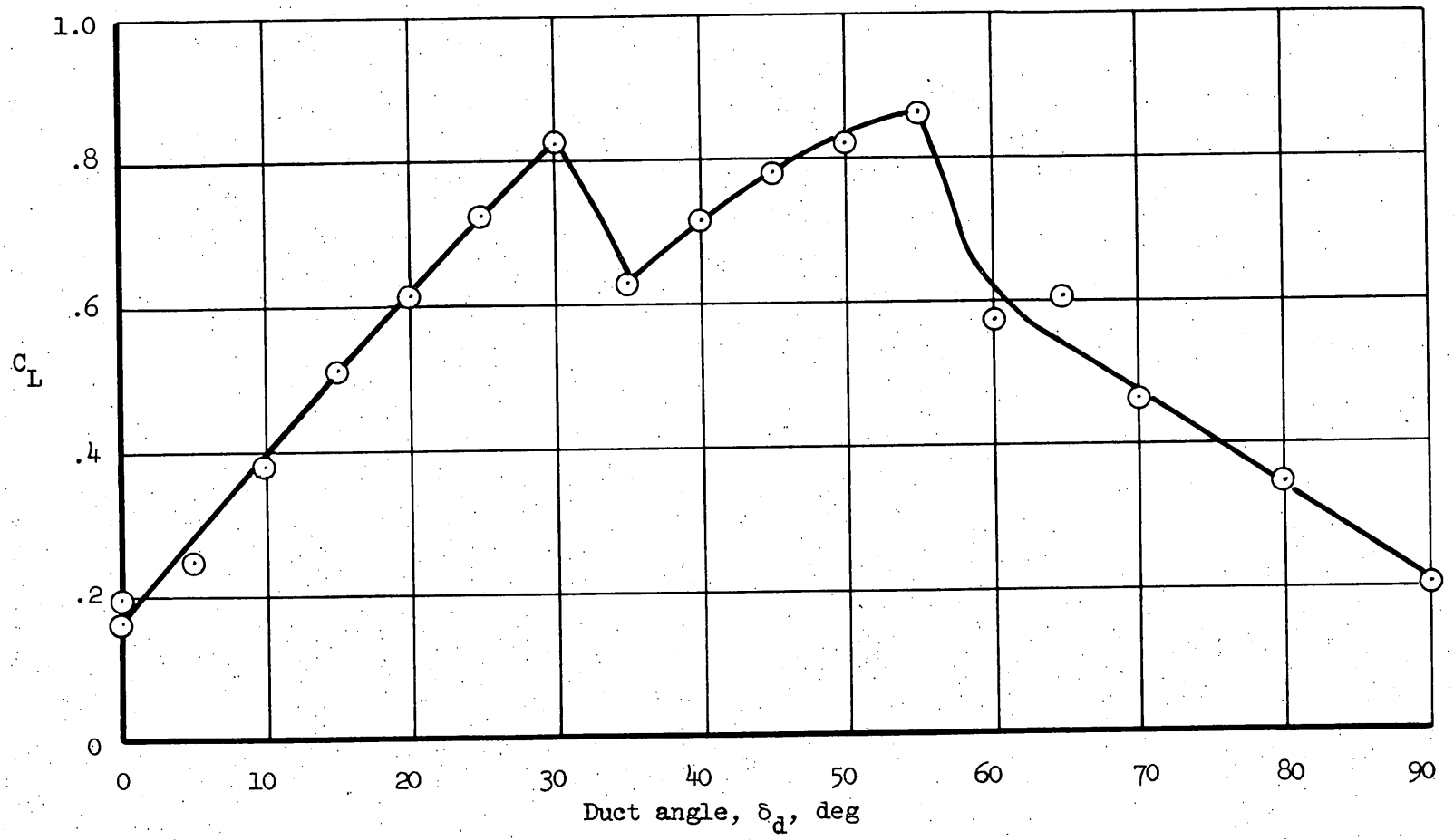

(a) Lift coefficient as a function of duct angle.

Figure 5.- Aerodynamic characteristics with the wing at 0° angle of attack; zero fan input power.

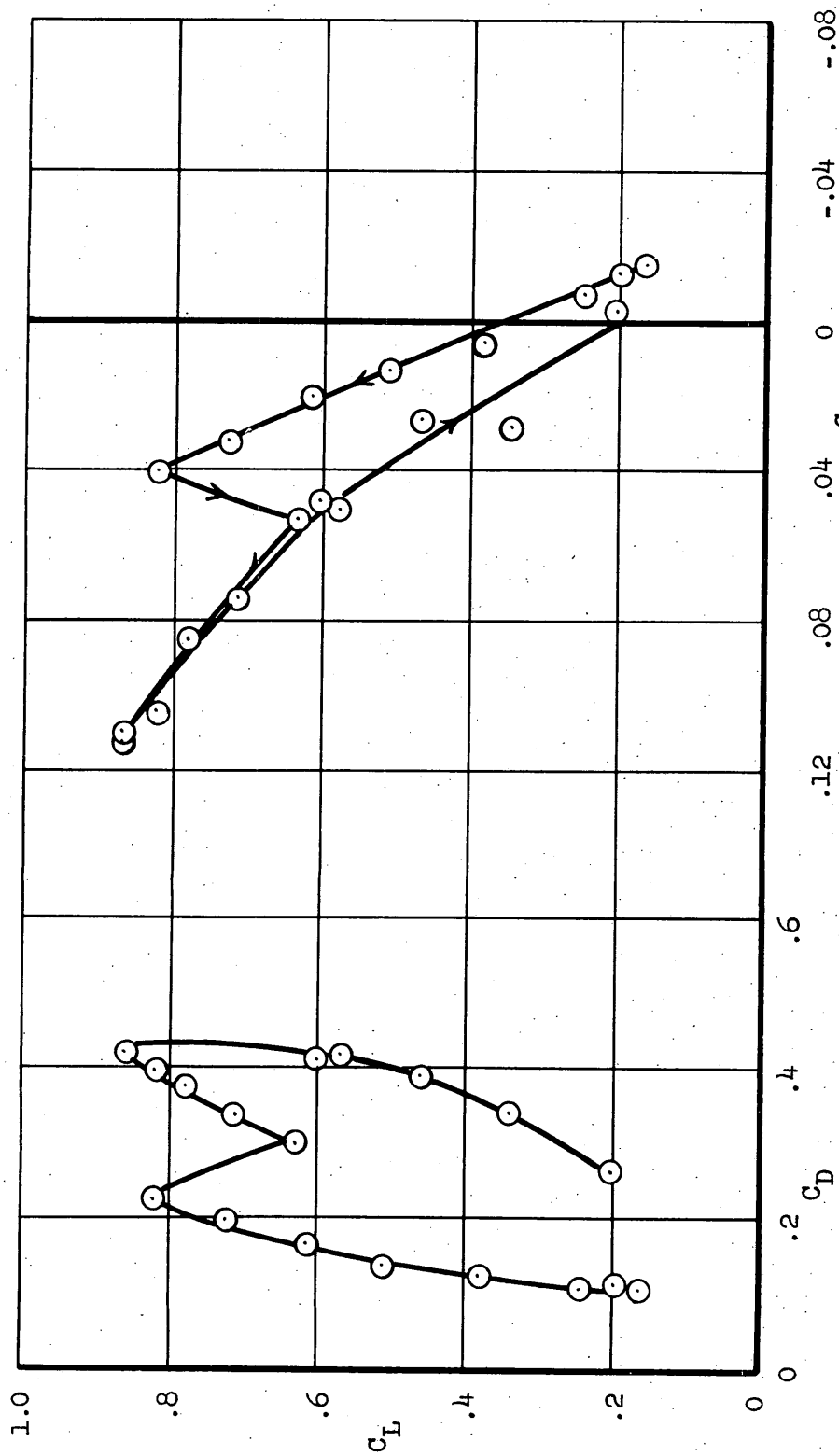

(b) Lift coefficient versus drag and pitching-moment coefficients.

Figure 5.- Concluded.

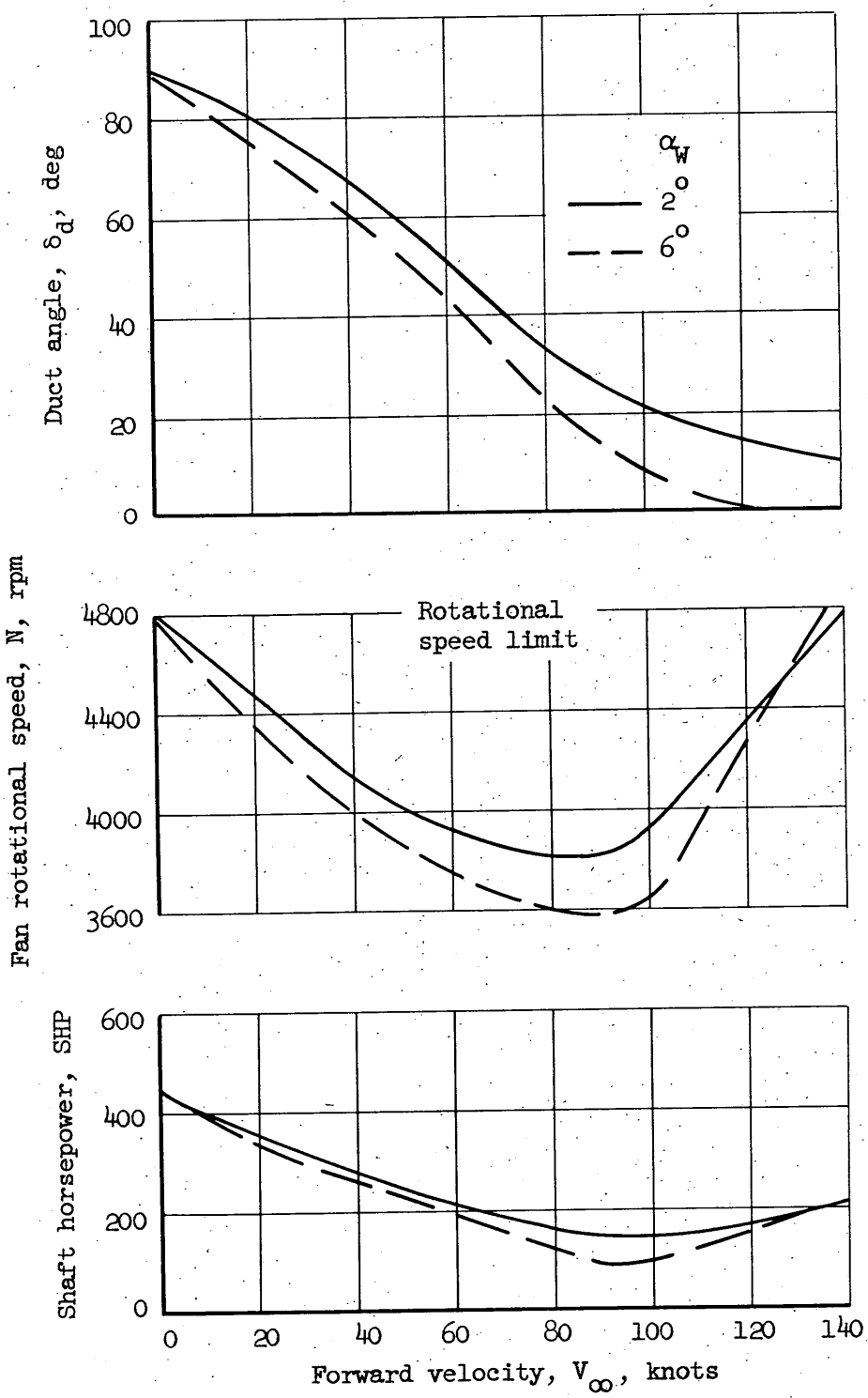

Figure 6.- Conditions for force balance of wing-duct combination for two wing angles of attack.

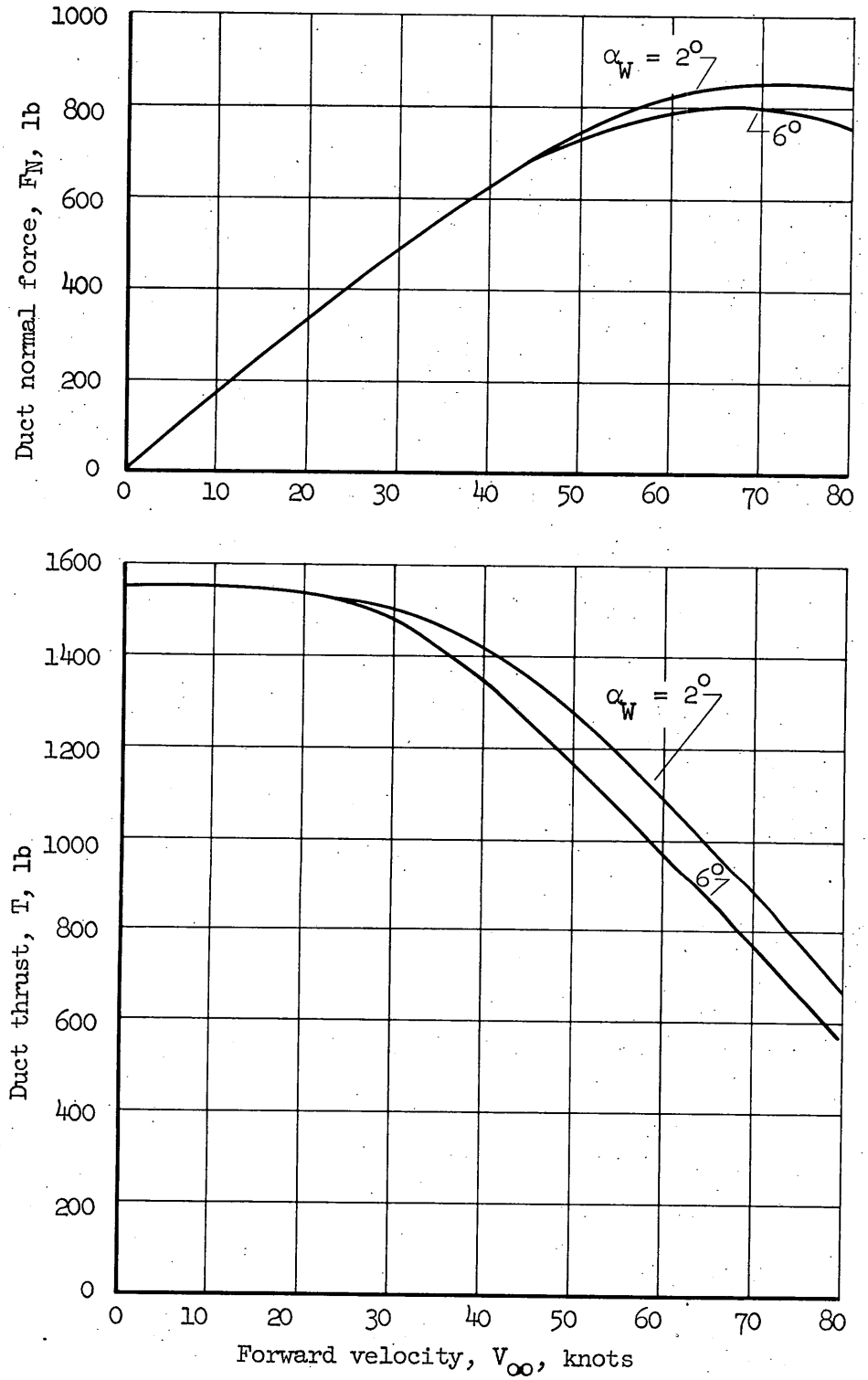

Figure 7.- Duct normal force and thrust as functions of forward velocity at force balance conditions for two wing angles of attack.

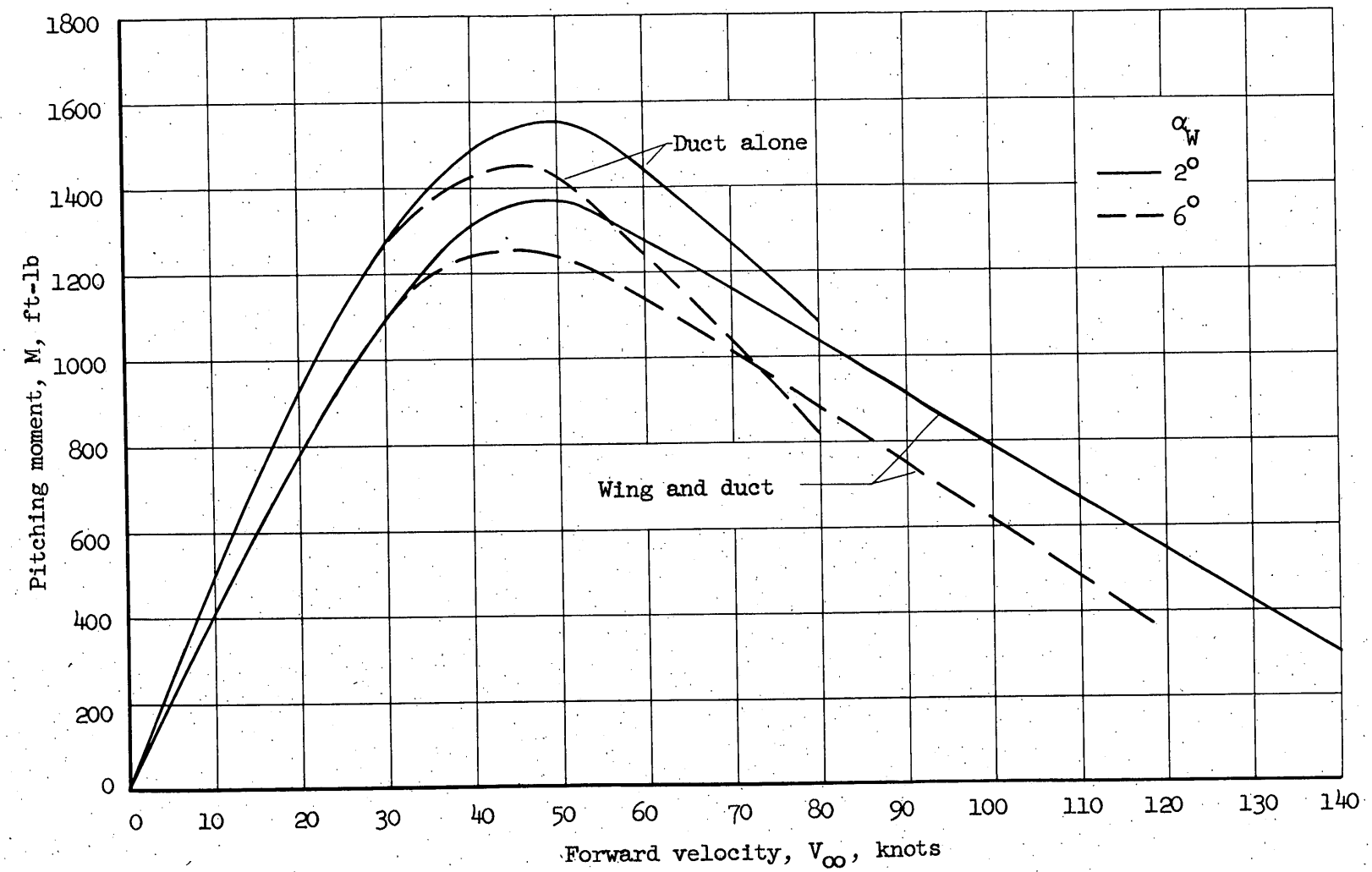

Figure 8.- Pitching moment as a function of forward velocity for two wing angles of attack.

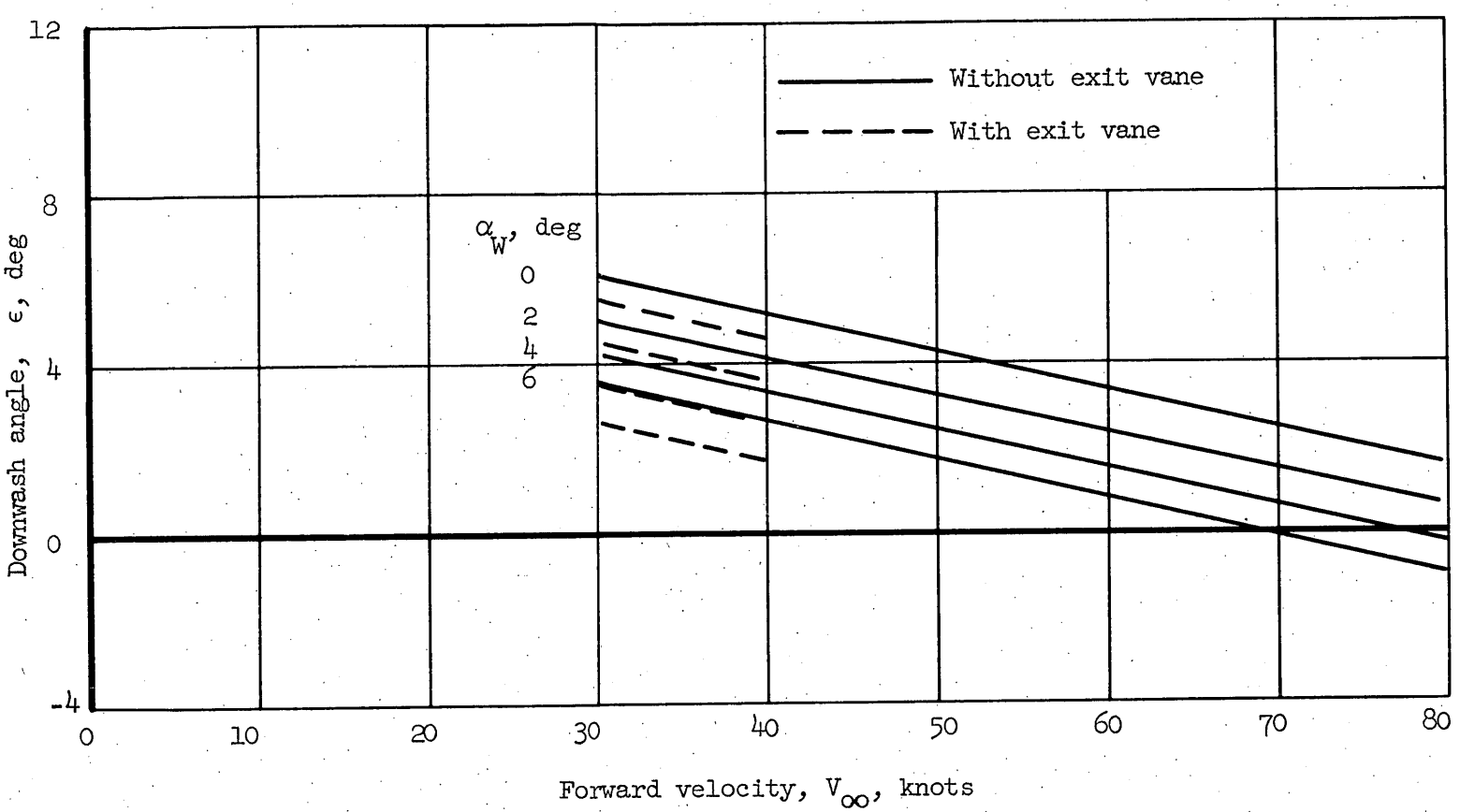

Figure 9.- Variation of the downwash angle at the chosen stabilizer location with forward velocity at several wing angles of attack.

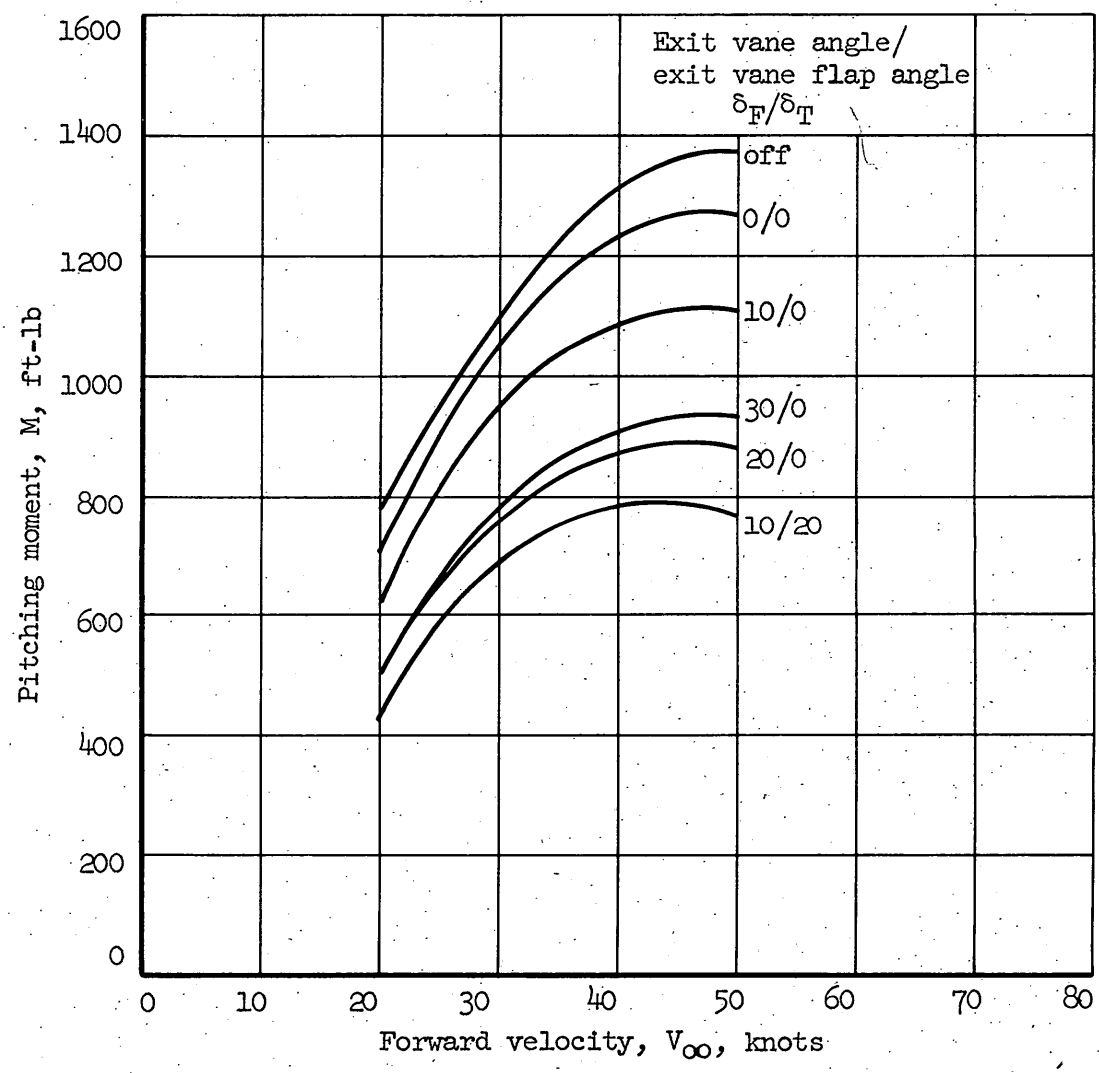

(a) Wing at 2° angle of attack.

Figure 10.- Wing-duct pitching moments at force balance conditions with the exit vane at various settings for two wing angles of attack.

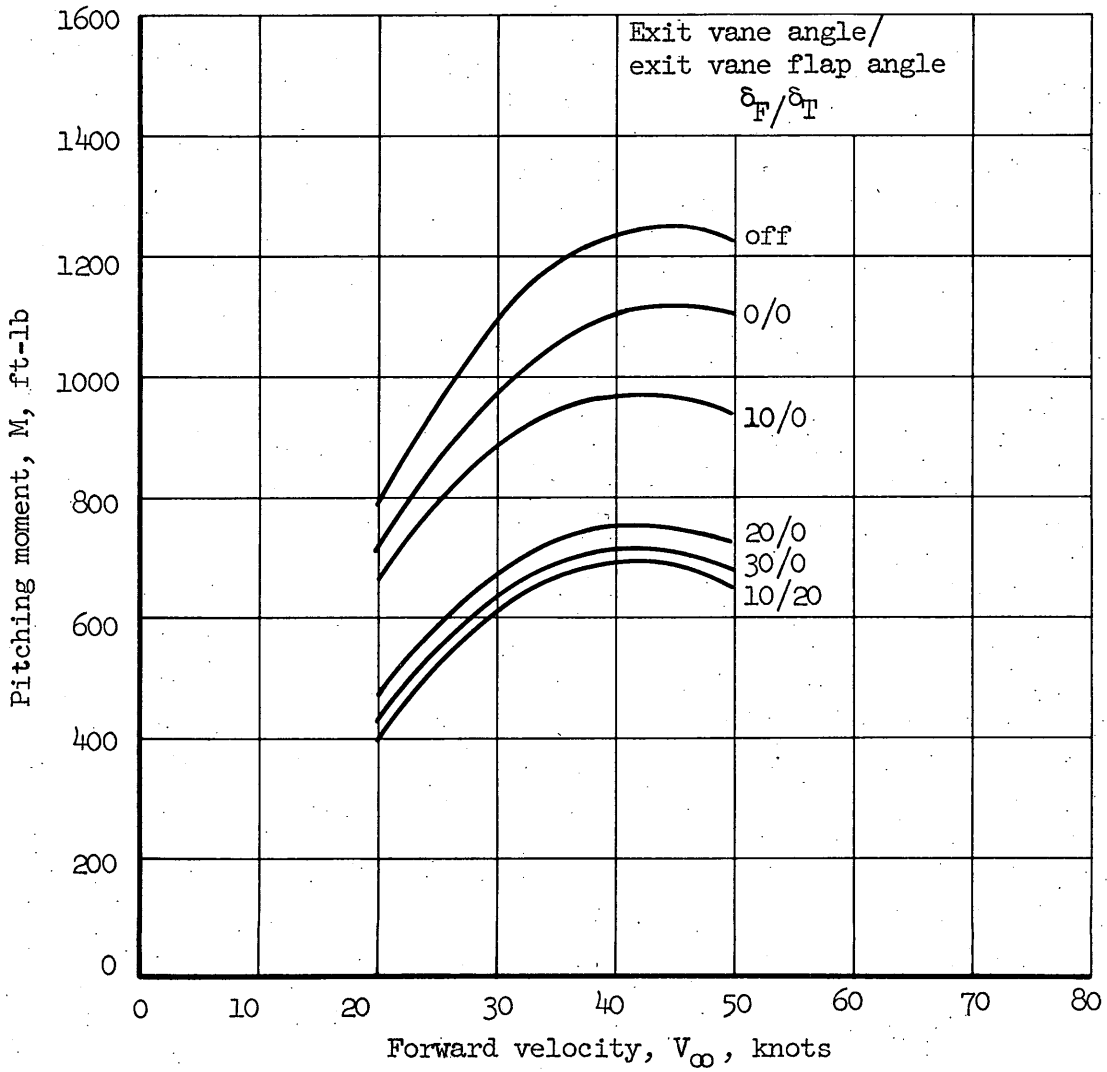

(b) Wing at 6° angle of attack.

Figure 10.- Concluded.

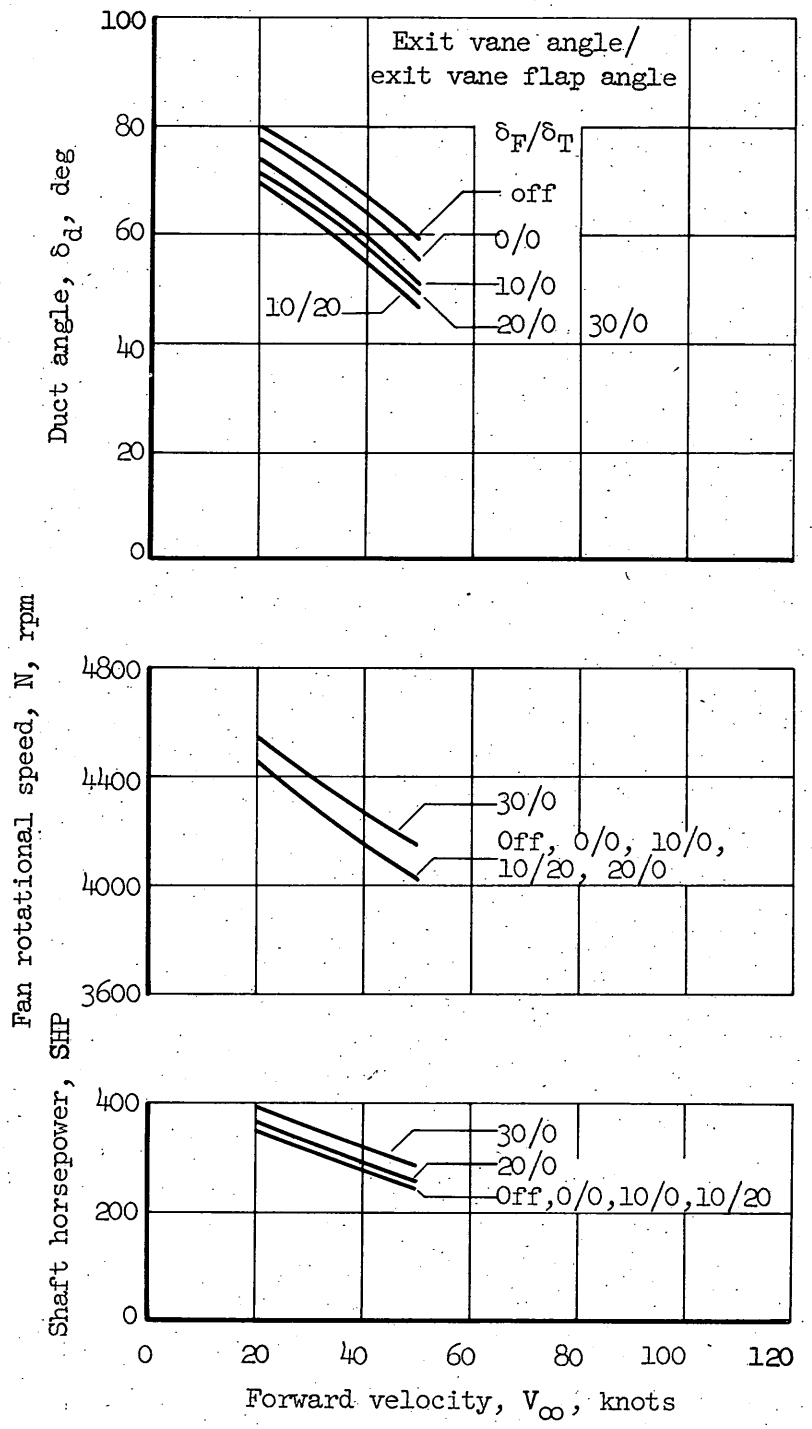

(a) Wing at 2° angle of attack.

Figure 11.- Duct angle, fan rotational speed, and shaft horsepower for force balance conditions as functions of forward velocity with the exit vane at various settings for two wing angles of attack.

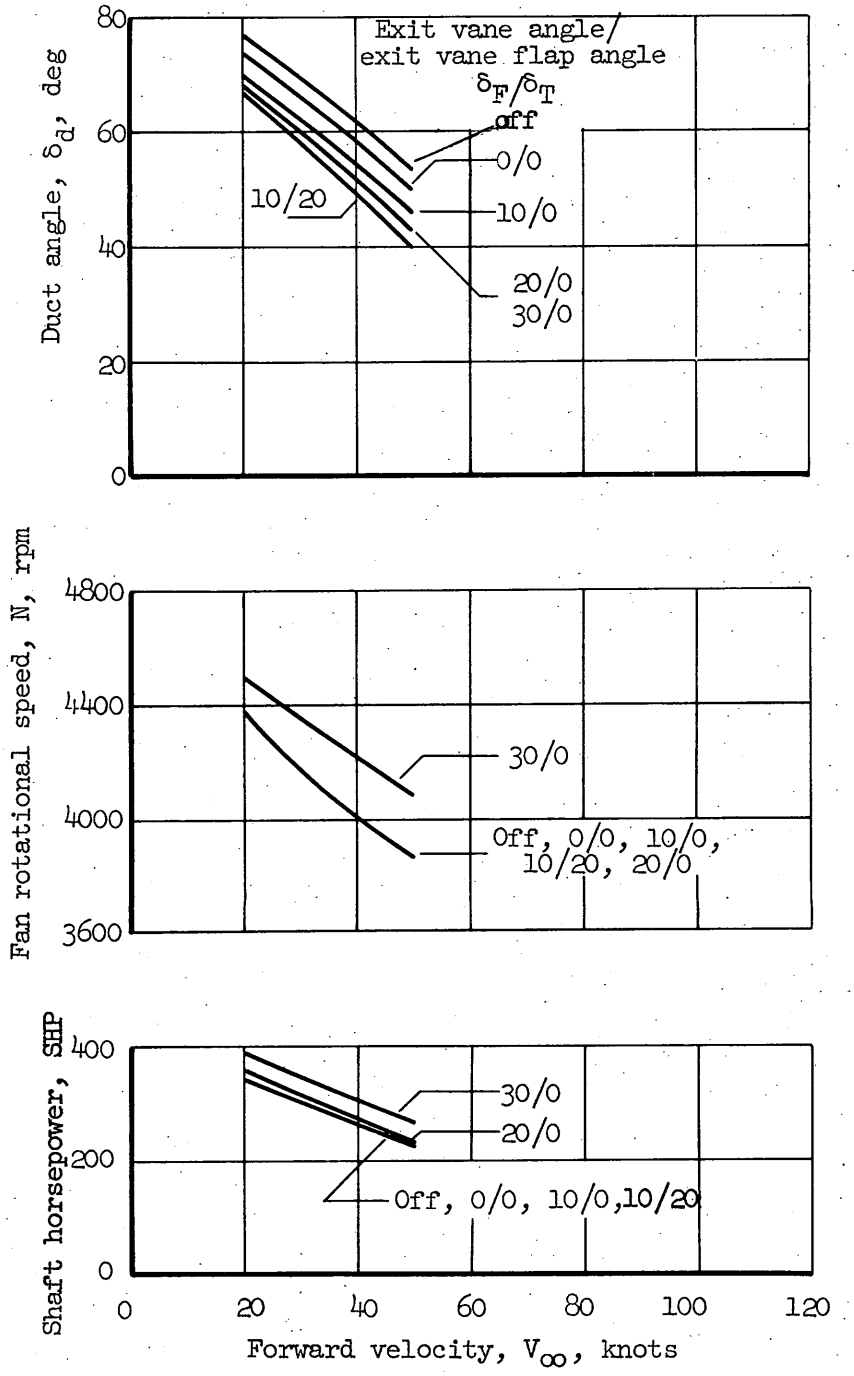

(b) Wing at 6° angle of attack.

Figure 11.- Concluded.

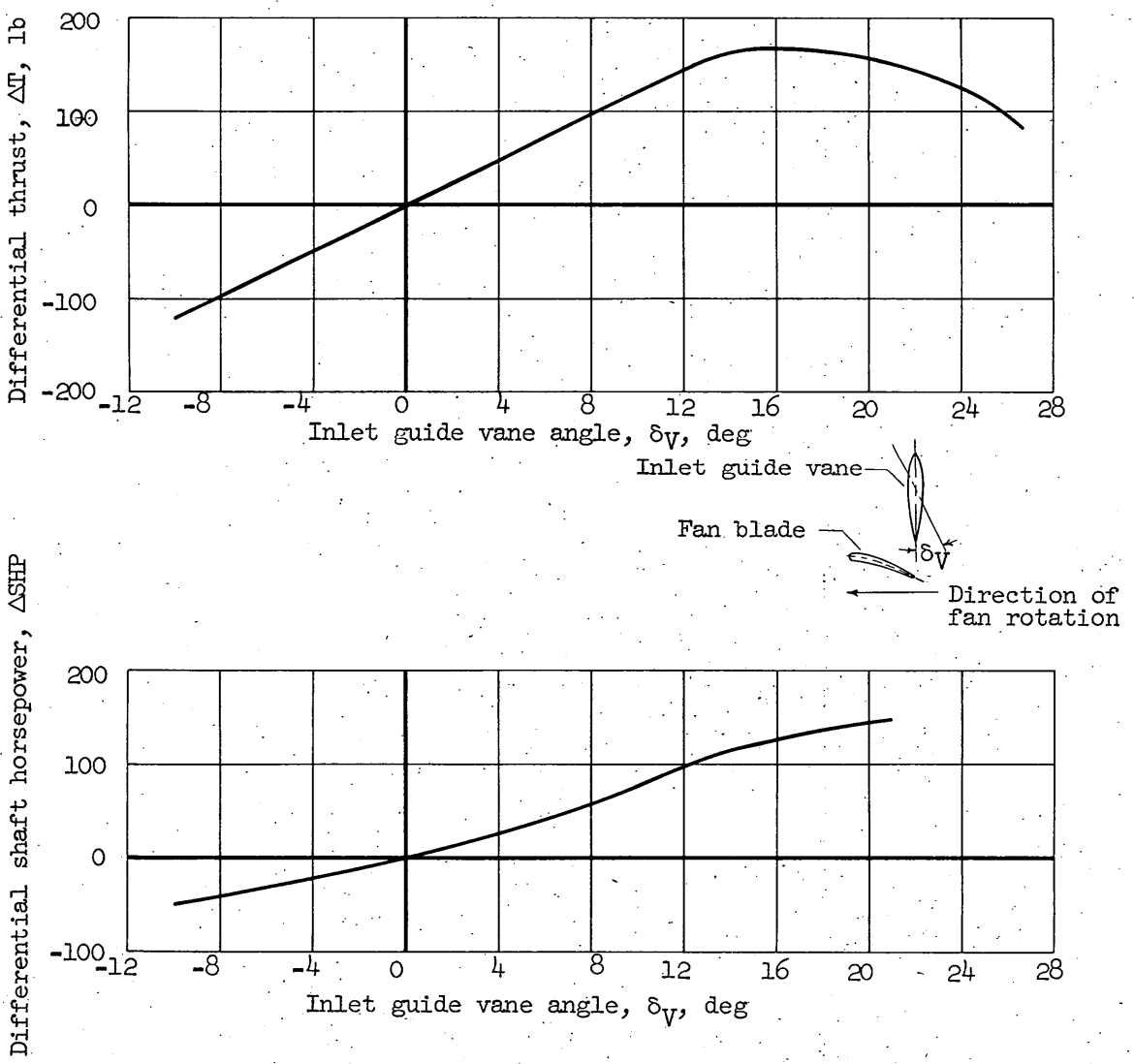

(a) Hover conditions; 14 inlet guide vanes.

Figure 12.- Differential thrust, ΔT, and differential shaft horsepower, ΔSHP, as functions of inlet guide vane angle; ΔT defined as thrust less thrust at zero inlet guide vane angle at force balance conditions; ΔSHP similarly defined.

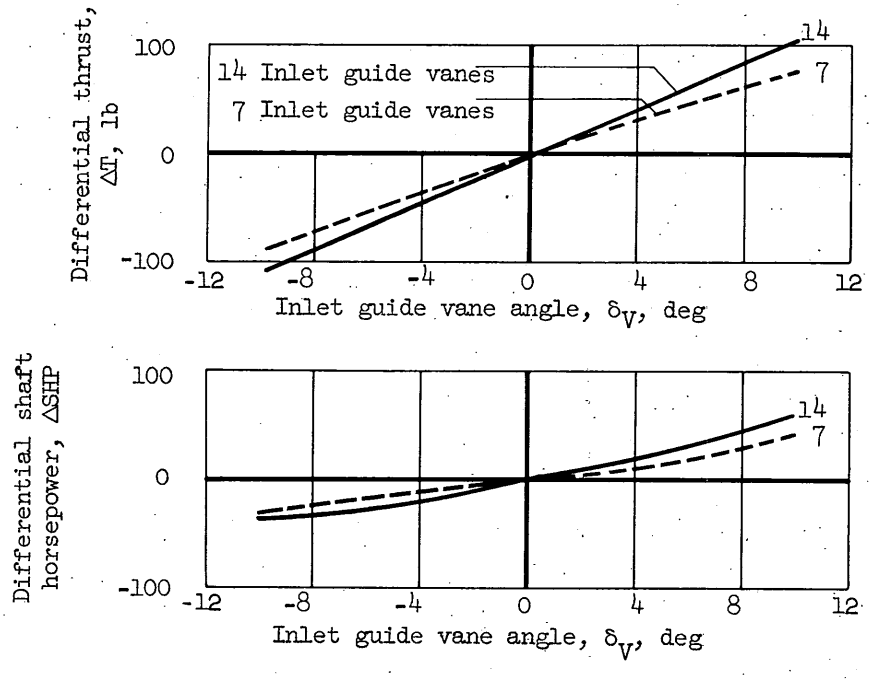

(b) Forward velocity, V_∞ = 20 knots.

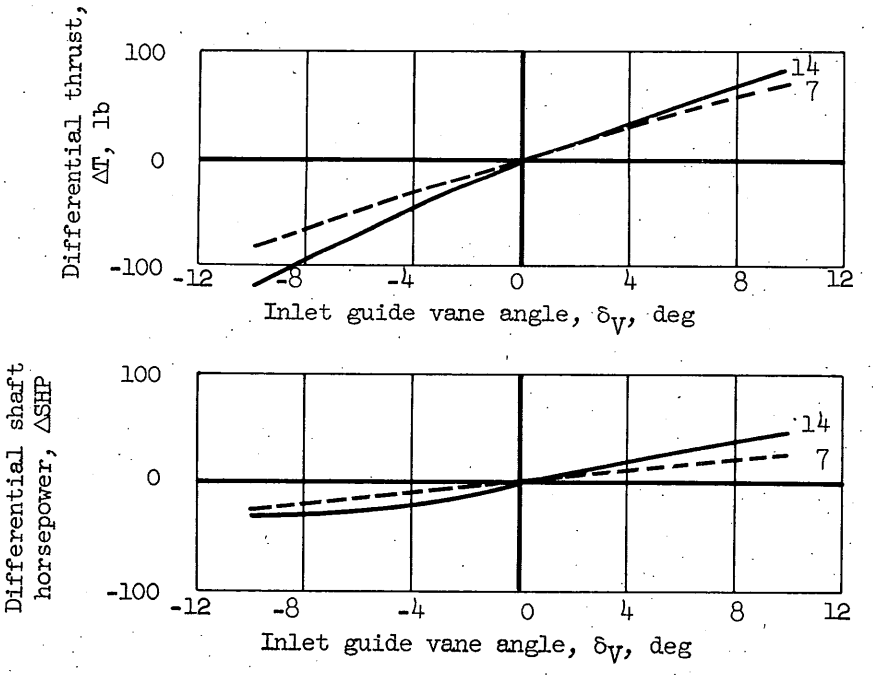

(c) Forward velocity, V_∞ = 30 knots.

Figure 12.- Concluded.